



Title	Intracellular disruption of mitochondria in a living HeLa cell with a 76-MHz femtosecond laser oscillator
Author(s)	Shimada, Tomoko; Watanabe, Wataru; Matsunaga, Sachihiko et al.
Citation	Optics Express. 2005, 13(24), p. 9869-9880
Version Type	VoR
URL	https://hdl.handle.net/11094/79048
rights	©2005 Optical Society of America. Users may use, reuse, and build upon the article, or use the article for text or data mining, so long as such uses are for non-commercial purposes and appropriate attribution is maintained. All other rights are reserved.
Note	

The University of Osaka Institutional Knowledge Archive : OUKA

<https://ir.library.osaka-u.ac.jp/>

The University of Osaka

Intracellular disruption of mitochondria in a living HeLa cell with a 76-MHz femtosecond laser oscillator

Tomoko Shimada and Wataru Watanabe

Department of Material and Life Science, Graduate School of Engineering, Osaka University
2-1, Yamadaoka, Suita, Osaka 565-0871, Japan
watanabe@photonics.mls.eng.osaka-u.ac.jp

Sachihiko Matsunaga, Tsunehito Higashi, Hiroshi Ishii, and Kiichi Fukui

Department of Biotechnology, Graduate School of Engineering, Osaka University
2-1, Yamadaoka, Suita, Osaka 565-0871, Japan

Keisuke Isoke and Kazuyoshi Itoh

Department of Material and Life Science, Graduate School of Engineering, Osaka University
2-1, Yamadaoka, Suita, Osaka 565-0871, Japan

Abstract: Femtosecond laser pulses can be used to selectively disrupt and dissect intracellular organelles. We report on disruption of mitochondria in living HeLa cells using a femtosecond laser oscillator with a repetition rate of 76 MHz. We studied the laser parameters used for disruption. The long-term viability of the cells after disruption of a single mitochondrion was confirmed by the observation of cell division, indicating that intracellular disruption of organelles using a femtosecond laser oscillator can be performed without compromising the long-term cell viability.

©2005 Optical Society of America

OCIS codes: (320.7110) Ultrafast nonlinear optics; (140.3440) Laser-induced breakdown; (170.0170) Medical optics and biotechnology; (170.1790) Confocal microscopy; (170.2520) Fluorescence microscopy; (180.1790) Confocal microscopy; (180.2520) Fluorescence microscopy; (190.7110) Ultrafast nonlinear optics

References and links

1. B. Alberts, D. Bray, A. Johnson, J. Lewis, M. Raff, K. Roberts, and P. Walter, *Essential Cell Biology* (Taylor and Francis, New York, 1997).
2. A. Ashkin, "Acceleration and trapping of particles by radiation pressure," *Phys. Rev. Lett.* **24**, 156-159 (1970).
3. R. L. Amy and R. Storb, "Selective mitochondrial damage by a ruby laser microbeam - an electron microscopic study," *Science* **150**, 756-757 (1965).
4. V. Venugopalan, A. Guerra III, K. Nahen, and A. Vogel, "Role of laser-induced plasma formation in pulsed cellular microsurgery and micromanipulation," *Phys. Rev. Lett.* **88**, 078103 (2002).
5. M. W. Berns, W. H. Write, and R. W. Steubing, "Laser microbeam as a tool in cell biology," *Int. Rev. Cytol.* **129**, 1-44 (1991).
6. J. Colombelli, S. W. Grill, and E. H. K. Stelzer, "Ultraviolet diffraction limited nanosurgery of live biological tissues," *Rev. Sci. Instrum.* **75**, 472-478 (2004).
7. J. Colombelli, E. G. Reynaud, J. Rietdorf, R. Pepperkok, E. H. K. Stelzer, "In vivo selective cytoskeleton dynamics quantification in interphase cells induced by pulsed ultraviolet laser nanosurgery," *Traffic* **6**, 1093-1102 (2005).
8. A. Khodjakov, R. W. Cole, and C. L. Rieder, "A synergy of technologies: Combining laser microsurgery with green fluorescent protein tagging," *Cell. Motil. Cytoskeleton* **38**, 311-317 (1997).
9. E. L. Botvinick, V. Venugopalan, J. V. Shah, L. H. Liaw, and M. W. Berns, "Controlled ablation of microtubules using a picosecond laser," *Biophys. J.* **87**, 4203-4212 (2004).
10. W. Denk, J. H. Strickler, and W. W. Webb, "Two-photon laser scanning fluorescence microscopy," *Science* **248**, 73-76 (1990).

11. K. König, P. T. C. So, W. W. Mantulin, and E. Gratton, "Cellular response to near-infrared femtosecond laser pulses in two-photon microscopes," *Opt. Lett.* **22**, 135-136 (1997).
12. K. König, T. W. Becker, P. Fischer, I. Riemann, and K. -J. Halbhuber, "Pulse-length dependence of cellular response to intense near-infrared laser pulses in multiphoton microscopes," *Opt. Lett.* **24**, 113-115 (1999).
13. J. M. Squirrell, D. L. Wokosin, J. G. White, and B. D. Bavister, "Long-term two-photon fluorescence imaging of mammalian embryos without compromising viability," *Nat. Biotechnol.* **17**, 763-767 (1999).
14. V. V. Yakovlev, "Advanced instrumentation for non-linear Raman microscopy," *J. Raman Spectrosc.* **4**, 957-964 (2003).
15. M. Lenzner, J. Krüger, S. Sartania, Z. Cheng, Ch. Spielmann, G. Mourou, W. Kautek, and F. Krausz, "Femtosecond optical breakdown in dielectrics," *Phys. Rev. Lett.* **80**, 4076-4079 (1998).
16. W. Watanabe, N. Arakawa, S. Matsunaga, T. Higashi, K. Fukui, K. Isobe, and K. Itoh, "Femtosecond laser disruption of subcellular organelles in a living cell," *Opt. Express* **12**, 4203-4213 (2004), <http://www.opticsexpress.org/abstract.cfm?URI=OPEX-12-18-4203>.
17. N. Shen, D. Datta, C. B. Schaffer, P. LeDuc, D. E. Ingber, and E. Mazur, "Ablation of cytoskeletal filaments and mitochondria in live cells using a femtosecond laser nanoscissor," *Mech. Chem. Biosyst.* **2**, 17-25 (2005).
18. A. Heisterkamp, I. Z. Maxwell, E. Mazur, J. M. Underwood, J. A. Nickerson, S. Kumar, and D. E. Ingber, "Pulse energy dependence of subcellular dissection by femtosecond laser pulses," *Opt. Express* **13**, 3690-3696 (2005), <http://www.opticsexpress.org/abstract.cfm?URI=OPEX-13-10-3690>.
19. M. F. Yanik, H. Cinar, H. N. Cinar, A. D. Chisholm, Y. Jin, and A. Ben-Yakar, "Functional regeneration after laser axotomy," *Nature* **432**, 822 (2004).
20. K. König, "Laser tweezers and multiphoton microscopes in life sciences," *Histochem. Cell Biol.* **114**, 79-92 (2000).
21. K. König, I. Riemann, and W. Fritzsche, "Nanodissection of human chromosomes with near-infrared femtosecond laser pulses," *Opt. Lett.* **26**, 819-821 (2001).
22. U. K. Tirlapur and K. König, "Targeted transfection by femtosecond laser," *Nature* **418**, 290-291 (2002).
23. W. Supatto, D. Débarre, B. Moulia, E. Brouzés, J. -L. Martin, E. Farge, and E. Beaupaire, "In vivo modulation of morphogenetic movements in Drosophila embryos with femtosecond laser pulses," *Proc. Natl. Acad. Sci. USA* **102**, 1047-1052 (2005).
24. L. Sacconi, I. M. Tolić-Nørrelykke, R. Antolini, and F. S. Pavone, "Combined intracellular three-dimensional imaging and selective nanosurgery by a nonlinear microscope," *J. Biomed. Opt.* **10**, 014002 (2005).
25. M. Müller, J. Squier, and G. J. Brakenhoff, "Measurement of femtosecond pulses in the focal point of a high-numerical-aperture lens by two-photon absorption," *Opt. Lett.* **20**, 1038-1040 (1995).
26. T. Higashi, E. Nagamori, T. Sone, S. Matsunaga, and K. Fukui, "A novel transfection method for mammalian cells using calcium alginate microbeads," *J. Biosci. Bioeng.* **97**, 191-195 (2004).
27. T. J. Collins and M. D. Bootman, "Mitochondria are morphologically heterogeneous within cells," *J. Exp. Biol.* **206**, 1993-2000 (2003).
28. C. L. Rieder and R. W. Cole, "Entry into mitosis in vertebrate somatic cells is guarded by a chromosome damage checkpoint that reverses the cell cycle when triggered during early but not late prophase," *J. Cell. Biol.* **142**, 1013-1022 (1998).
29. C. L. Rieder and R. Cole, "Microtubule disassembly delays the G2-M transition in vertebrates," *Curr. Biol.* **10**, 1067-1070 (2000).
30. C. Xu and W. W. Webb, "Measurement of two-photon excitation cross sections of molecular fluorophore with data from 690 to 1050nm," *J. Opt. Soc. Am. B.* **13**, 481-491 (1996).
31. G. A. Blab, P. H. M. Lommerse, L. Cognet, G. S. Harms, and T. Schmidt, "Two-photon excitation action cross-sections of the autofluorescent proteins," *Chem. Phys. Lett.* **350**, 71-77 (2001).
32. A. P. Joglekar, H. H. Liu, E. Meyhöfer, G. Mourou, and A. J. Hunt, "Optics at critical intensity: Applications to nanomorphing," *Poc. Natl. Acad. Sci. USA* **101**, 5856-5861 (2004).
33. A. Vogel, J. Noack, G. Huettmann, and G. Paltauf, "Femtosecond-laser-produced low-density plasmas in transparent biological media: a tool for the creation of chemical, thermal, and thermomechanical effects below the optical breakdown threshold," *Proc. SPIE* **4633**, 23-37 (2002).
34. A. Schnle and S. W. Hell, "Heating by absorption in the focus of an objective lens," *Opt. Lett.* **23**, 325-327 (1998).
35. H. Oehring, I. Riedmann, P. Fisher, K. J. Halbhuber, and K. König, "Ultrastructure and reproduction behaviour of single CHO-K1 cells exposed to near infrared femtosecond laser pulses," *Scanning* **22**, 263-270 (2000).
36. U. K. Tirlapur, K. König, C. Peuckert, R. Krieg, and K. Halbhuber, "Femtosecond near-infrared laser pulse elicit generation of reactive oxygen species in mammalian cells leading to apoptosis-like death," *Exp. Cell Res.* **263**, 88-97 (2001).
37. A. Musacchio and K. G. Hardwick, "The spindle checkpoint: structural insights into dynamic signaling," *Nat. Rev. Mol. Cell Biol.* **3**, 731-741 (2002).

38. D. Arnoult, A. Grodet, Y. -J. Lee, J. Estaquier, and C. Blackstone, "Release of OPA1 during apoptosis participates in the rapid and complete release of cytochrome c and subsequent mitochondrial fragmentation," *J. Biol. Chem.* **280**, 35742-35750 (2005).
-

1. Introduction

The study of cell dynamics, such as mitosis, metabolism, and apoptosis, is of great importance to understand the biological and developmental properties of cells [1]. Lasers have been used for imaging cellular structures noninvasively, as well as for manipulating intact organelles in living cells. For example, optical tweezers have been used for manipulation of cells and subcellular organelles in three dimensions [2].

Another application of lasers is intracellular surgery, whereby a focused laser beam allows the function of organelles to be controlled without physically touching them. This laser surgery technique has been applied to disruption and dissection of intracellular structures. The light sources typically used for laser surgery are continuous (CW) lasers, nanosecond pulsed lasers, and picosecond pulsed lasers in the ultraviolet (UV) and visible regions [3-9]. UV lasers have some disadvantages, namely, their low light penetration depth, collateral damage outside the focal volume, the risk of photo-damage to living cells due to absorption, and the induction of oxidative stress leading to apoptosis. A focused nanosecond-pulse laser beam causes thermal damage and denaturation of the protein molecules around the laser focus. The main disadvantage of using UV and visible lasers is that the viability of the cells after laser irradiation is relatively low.

To overcome these problems, near-infrared femtosecond lasers have recently attracted much attention. Femtosecond lasers can be used to image subcellular structures using multiphoton excitation microscopy [10] without compromising viability [11-14]. Femtosecond lasers can also be used to perform laser nanosurgery at higher energies. Because there are virtually no efficient cellular absorbers in the 700-1100 nm spectral region, there is no photo-damage outside the focal volume. Additionally, a femtosecond laser pulse can produce localized energy absorption because the pulse width is shorter than the time required for heat to diffuse out of the focal volume [15] and ablation occurs only in and around the focal volume. Thus, femtosecond laser surgery has become an important tool for disruption or dissection of organelles on a scale of hundreds of nanometers to micrometers.

Femtosecond laser surgery has been demonstrated by use of both low-repetition-rate (1 kHz to 250 kHz) amplified Ti:sapphire laser systems and high-repetition-rate Ti:sapphire oscillators (~80 MHz). Amplified systems can provide high pulse energy and cause less thermal damage due to the low repetition rate. Several groups have recently reported femtosecond laser surgery using regenerative amplifiers with pulse energies of a few nanojoules to a few tens of nanojoules, disruption of mitochondria in living cells [16,17], dissection of actin fiber bundles [17], ablation of nuclei in fixed endothelial cells, ablation of single microtubules in living cells [18], and dissection of axons [19].

Although amplified Ti:sapphire laser systems produce high energy laser pulses, they are complex and expensive. In contrast, femtosecond oscillators are more compact and less expensive. A femtosecond oscillator can contribute to the construction of integrated systems with dual outputs for nonlinear imaging, including multiphoton microscopy and higher harmonic generation microscopy, as well as laser surgery. In particular, the use of a femtosecond oscillator enables laser surgery with low pulse energy in the sub-nanojoule region. For these reasons, several researchers have adopted femtosecond laser oscillators for nanosurgery of cells and cellular organelles [20-24]. Examples include knocking out single organelles in living cells [22], ablation in *Drosophila* embryos to induce modulation of specific movements [23], and the combination of two-photon microscopy and nanosurgery of fluorescent structures within yeast mitotic spindles [24]. Of particular interest is laser surgery of mitochondria because mitochondria play key roles in energy production, cell death processes (apoptosis), and subcellular homeostasis. For example, knocking-out of a mitochondrion using a femtosecond laser oscillator has been reported [20]. However, laser

parameters for disruption have not been investigated in detail, nor has the loss of long-term viability after disruption been reported.

In this paper, we report on the disruption of mitochondria in living HeLa cells by focusing femtosecond laser pulses produced by a Ti:sapphire laser oscillator. Laser parameters for disruption of the mitochondria are investigated. The long-term viability of the cells is confirmed by the observation of cell division after disruption of individual mitochondria.

2. Experimental setup

Figure 1 shows a schematic diagram of the setup used for the disruption of fluorescence-labeled organelles in living cells using a femtosecond laser oscillator. Details of the confocal laser-scanning microscope used here to visualize organelles in the living cells were reported in Ref. 16. The laser scanning microscope was adapted from an Olympus FV300 scanning unit combined with an Olympus IX71 inverted microscope. A collimated CW laser beam of a He-Ne laser (wavelength 543 nm) or an Ar-ion laser (wavelength 488 nm) was reflected by dichroic mirrors DM1 and DM2 and then focused into the cells through an oil-immersion objective lens (OB; Olympus Corporation, PlanApo60×Oil, NA 1.4). The back-propagated one-photon fluorescence was collected using the same objective lens and detected with photomultiplier tubes (PMT1 and PMT2; Hamamatsu Photonics, R928P). Bandpass filters BP1 (transmission wavelength: 510 nm - 540 nm) and BP2 (transmission wavelength: 560 nm - 600 nm) were placed before PMT1 and PMT2. Two-dimensional confocal cross-sectional images were obtained by scanning the focused laser beams in the xy plane with a pair of high-speed galvanometer mirrors (GM; Cambridge, 6210) inside the laser-scanning microscope. Scanning in the depth direction (z direction) was achieved by moving the objective lens with a stepping motor to obtain three-dimensional confocal images.

Irradiation with femtosecond laser pulses was performed using a mode-locked Ti:sapphire laser oscillator with a wavelength of 800 nm and a repetition rate of 76 MHz (Coherent, Mira). The laser pulses passed through a Faraday isolator (FI) to block reflections from the optical components. The laser pulses then passed through a series of SF10 prisms (P1, P2) to compensate for the dispersion of the optical components in the light path and the microscope. To fill the aperture of the objective lens (OB), the beam was reduced to 2 mm in diameter with a pair of lenses (L1, L2), and it was then directed onto a pair of GM via DM1 and DM2. Femtosecond laser pulses were focused into the cells through the oil-immersion objective. To determine the pulse width of the femtosecond laser pulses at the sample, two-photon absorption (TPA) autocorrelation was employed [25]. A Michelson interferometer (not shown in Fig.1) was placed before DM1. The reflected laser beam via M3 was directed into the Michelson interferometer and the beam was split into two beams with a beam splitter. The combined beam returning from the interferometer was fed into the laser scanning microscope. Two beams were focused into 3 mM solutions of Rhodamine 6G (Molecular Probes) dissolved in ethanol by the objective lens instead of a biological sample. The returning two-photon fluorescence was epi-detected by the PMT1 after passing through a filter BP1 to block the excitation wavelength of the Ti:sapphire laser pulses. Changing the path length in one arm of the interferometer allowed determination of the second-order autocorrelation of the pulses. From the TPA interferometric autocorrelation function, the pulse duration measured at the specimen through the microscope was 145 fs (full width at half maximum), assuming a Gaussian pulse.

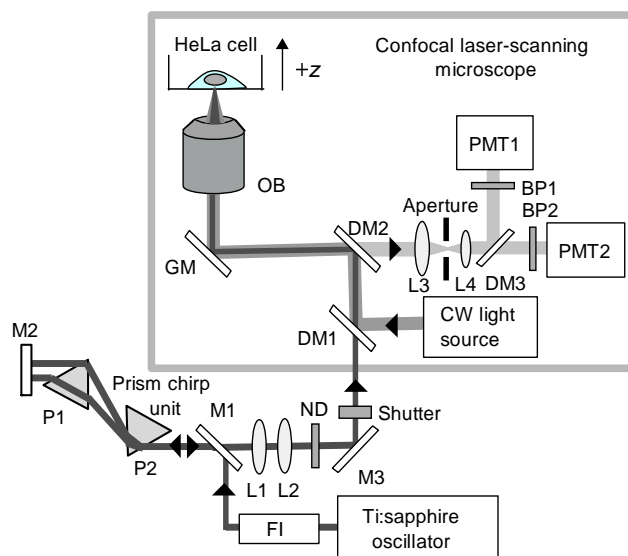


Fig. 1. Schematic diagram of the experimental setup. FI, Faraday isolator; P, SF10 prism; M mirror; L, lens; ND, neutral density filter; DM, dichroic mirror; OB, objective lens; GM, pair of galvanometer mirrors; PMT, photomultiplier tube

HeLa human carcinoma cells were cultured and maintained as previously reported [16, 26]. For visualization of the chromosomes, the HeLa cells were transfected by pEGFP-C1/histone H1.2 using LipofectAMINE plus reagent (Invitrogen). Cell cycle synchronization was performed by incubating the cells with 2.5 mM thymidine for 20 h. Cells were then washed three times and incubated in fresh media without thymidine.

3. Disruption of mitochondria

We now show the disruption of individual mitochondria in living HeLa cells using the femtosecond laser oscillator system described above. The cells expressed the enhanced yellow fluorescent protein (EYFP) in the mitochondria. Stacked three-dimensional confocal images of cells were observed by excitation with the Ar^+ laser, as shown in Fig. 2(a). To produce a stacked 3D image, nine confocal cross-sectional images were obtained by translating the objective lens by $2\ \mu\text{m}$ in the depth (z) direction in steps of 250 nm. Figure 2(c) shows a series of confocal cross-sections obtained along the depth direction. The images are magnified views of the mitochondria around the focal spot. A train of femtosecond laser pulses with an energy of 0.39 nJ/pulse was focused and the shutter was open for an exposure time of 32 ms, which corresponded to 2.4×10^6 pulses. The time duration necessary to obtain two stacked confocal images before and after femtosecond laser irradiation was 30 seconds. Figure 2(b) shows the stacked confocal image obtained after femtosecond laser irradiation, and Fig. 2(d) shows a series of magnified cross-sections of the mitochondria. Figures 2 shows that fluorescence from a 5- μm -long single mitochondrion disappeared. Displacement of the mitochondria outside the focal region between the before and after images was attributed to cytoplasmic streaming, which indicated the viability of the cells.

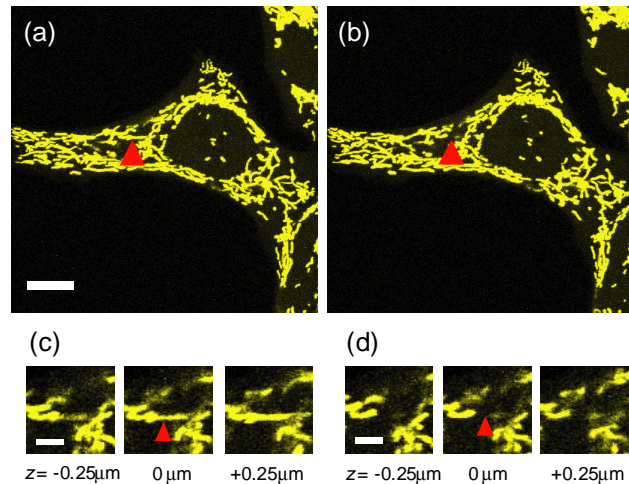


Fig. 2. Stacked three-dimensional confocal images (a) before and (b) after femtosecond laser irradiation with 0.39 nJ/pulse (exposure time: 32 ms). Stacked images were obtained by translating the objective lens by 1 μm in the depth direction in steps of 250 nm. Yellow fluorescence shows mitochondria of HeLa cells visualized by EYFP. A target mitochondrion is indicated by a red arrow. Scale bar: 10 μm . Confocal cross-sectional images at different depths (c) before and (d) after irradiation of the femtosecond laser pulses. The femtosecond laser pulses were focused at a depth of $z = 0$. Scale bar: 3 μm .

To confirm that disappearance of fluorescence after focusing femtosecond laser pulses is due to disruption, rather than bleaching of the fluorophore, restaining and transmission electron microscopy (TEM) are generally used. TEM analysis is useful for fixed cells; however, it cannot be directly applied to living cells [18]. On the other hand, the restaining method is feasible for living cells [16,19]. We examined the effectiveness of the restaining method in combination with fluorescence recovery after photobleaching (FRAP) analysis. Here, we used the enhanced green fluorescent protein (EGFP) labeled nucleus. An EGFP labeled nuclear region of $1.5 \times 1.5 \mu\text{m}^2$ in a living HeLa cell was irradiated while varying the femtosecond laser energy (0.21, 0.26, and 0.39 nJ/pulse) at a wavelength of 925 nm. We used the wavelength of 925 nm because the efficiency of two-photon absorption at this longer wavelength is higher than that at 800 nm. An exposure time of 1.1 s for scanning the nuclear region of $1.5 \times 1.5 \mu\text{m}^2$ was used to clearly discern disruption or bleaching. Time-lapse images of the nucleus were acquired by excitation with the Ar^+ laser before and after femtosecond laser irradiation. At the energies of 0.21 and 0.26 nJ/pulse, the fluorophore was bleached, and subsequent recovery of fluorescence in the bleached region occurred due to inward diffusion of unbleached fluorophore molecules. The time required for 50% recovery of fluorescence was 20 s. At the energy of 0.39 nJ/pulse, fluorescence in the focal region disappeared; however, fluorescence recovery was not observed in this case. After femtosecond laser irradiation, we restained the same cell with a blue fluorophore (Hoechst 33342). Because nuclei normally became suitably stained 40 min after the addition of Hoechst 33342, we obtained fluorescence images after 45 minutes. When the bleaching occurred, fluorescence was also observed from both EGFP and Hoechst 33342. When disruption of the nucleus occurred, no fluorescence was observed from EGFP or Hoechst 33342 in the laser-irradiated region. These results demonstrate that observation of fluorescence recovery is an indicator of the disruption of organelles in living cells.

We confirmed disruption of the mitochondrion in the case shown in Fig. 2 using the previously reported restaining method [16]. The EYFP in the mitochondria onto which the femtosecond laser pulses were focused was not restained with MitoTracker Red. Previous

FRAP experiments on mitochondria showed that the time required for 50% recovery of fluorescence was a few seconds [27]. We could not directly measure the threshold energy for bleaching and disruption when targeting mitochondria because the time duration between the two images before and after irradiation was 10 s in our system. Since the mitochondria irradiated by the femtosecond laser pulses in our experiments did not exhibit fluorescence recovery after 30 s, the mechanism must be different from bleaching. We have therefore shown that disruption and bleaching are distinguishable using FRAP analysis and the restaining method.

When laser pulses with higher energy were focused into the mitochondria, changes in the mitochondrial morphology were observed. After irradiating the matrix of a single mitochondrion using a pulse energy of 0.53 nJ/pulse (exposure time: 32 ms), tubular mitochondria became fragmented into punctiform. Figure 3 shows an example of mitochondrial fragmentation. Figures 3(a) and (b) show the stacked three-dimensional confocal images obtained before and after femtosecond laser irradiation. In addition to the target mitochondrion, peripheral mitochondria were also disrupted and the morphology of the mitochondria changed. Tubular mitochondria became 1- μm -long fragmented mitochondria 500 s after irradiation [Fig. 3(c)]. Therefore, the higher energies are not suitable for selective disruption of targeted mitochondria.

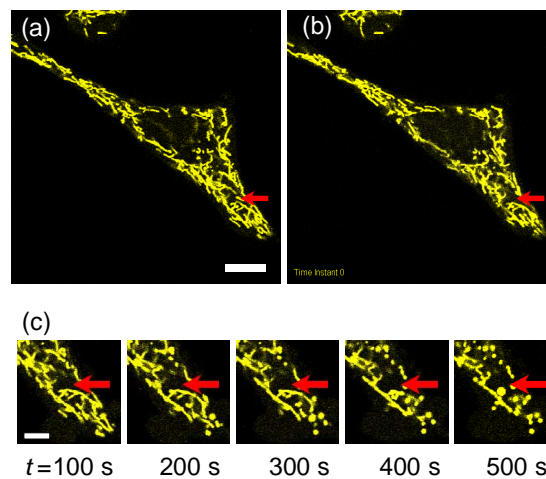


Fig. 3. Mitochondrial fragmentation in HeLa cells induced by femtosecond laser pulses. Stacked three-dimensional confocal images obtained (a) before and (b) after irradiation with 0.53 nJ/pulse (exposure time: 32 ms). The red arrow indicates the irradiation point. Scale bar: 10 μm . (c) Time-lapse confocal images after irradiation. Scale bar: 5 μm .

In femtosecond laser surgery of organelles in living cells, it is important to use the optimal laser parameters. To this end, we investigated how the efficiency of mitochondrion disruption depended on the pulse energy and the irradiation time. We compared the fluorescence images before and after femtosecond laser irradiation. The time duration between the two images was 10 s. We performed all the experiments in Fig. 4 at the energies of 0.32 nJ, 0.37 nJ, 0.42 nJ, 0.47 nJ, 0.53 nJ, 0.66 nJ, and 0.79 nJ. Ten measurements were performed at each pulse energy and irradiation time. The experimental results presented in Figs. 4(a) to (c) were performed with EYFP-mitochondria. Figure 4(a) shows the rate of disruption and fragmentation of mitochondria for an irradiation time of 32 ms at various laser energies. When the pulse energy was 0.40 ± 0.14 nJ/pulse, the single target mitochondrion was disrupted without affecting neighboring mitochondria. The energy variance was attributed to cell activity in living cells. Above 0.5 nJ/pulse, fragmentation of mitochondria occurred. Figures 4(b) and (c) show the rates of disruption and fragmentation of mitochondria for irradiation times of 16 ms

and 8 ms, respectively. The energies for disruption of the mitochondria were 0.46 ± 0.14 nJ/pulse for the irradiation time of 16 ms and 0.63 ± 0.3 nJ/pulse for the irradiation time of 8 ms. Experiments showed that a shorter irradiation time required higher disruption energy. Next, we investigated the rate of disruption of mitochondria stained with MitoTracker Red at the irradiation time of 32 ms. The energy for disruption of mitochondria stained with MitoTracker Red was 0.46 ± 0.14 nJ/pulse [Fig. 4 (d)].

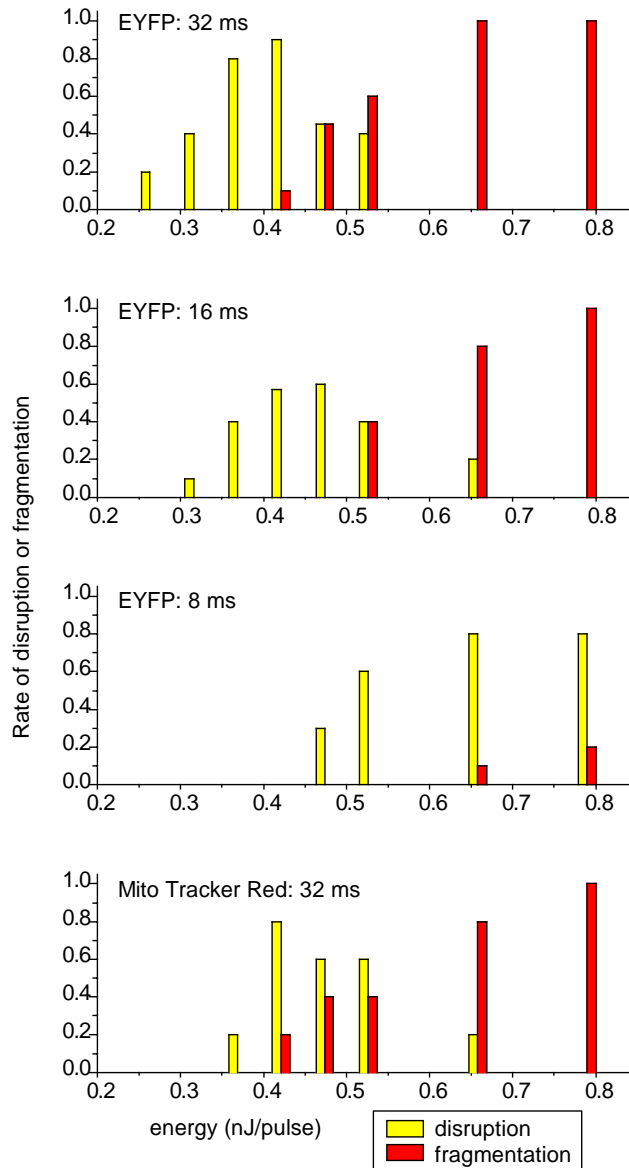


Fig. 4. Dependence of disruption of mitochondria with EYFP and MitoTracker Red on femtosecond laser pulse energy and irradiation time. (a-c) The rate of disruption and fragmentation of the EYFP-mitochondria at irradiation times of (a) 32 ms, (b) 16 ms, and (c) 8 ms for various laser energies. (d) The rate of disruption and fragmentation of the mitochondria stained with MitoTracker Red at an irradiation time of 32 ms for various laser energies. The number of measurements was 10 for each pulse energy and irradiation time.

4. Viability of Cells after femtosecond laser surgery

It is important in laser surgery not to compromise the viability of cells. Several researchers reported that entry into mitosis was guarded by a checkpoint that could be activated by a variety of insults, including chromosomal damage and disrupting microtubules using UV laser light or drugs [28,29]. We investigated the viability of the cells after disruption of a mitochondrion by observing cell division.

In our primary experiment, we identified interphase cells. In this experiment, mitochondria in the HeLa cells were visualized by EYFP without synchronization and incubated at 37°C in a temperature-controlled incubator (Tokken) on the microscope stage. Figure 5 shows cell division after disruption of a mitochondrion. Figures 5(a) and (b) show the disruption of a targeted mitochondrion before and after irradiation with femtosecond laser pulses at an energy of 0.39 nJ /pulse (exposure time: 32 ms). The cell was alive because cytoplasmic streaming in the cell was continuously observed. The process of cell division finished successfully 12 h after laser irradiation [Fig. 5(c)]. Moreover, the migration of daughter cells was observed from 12 to 16.5 h after laser irradiation [Figs. 5(c) to (b)].

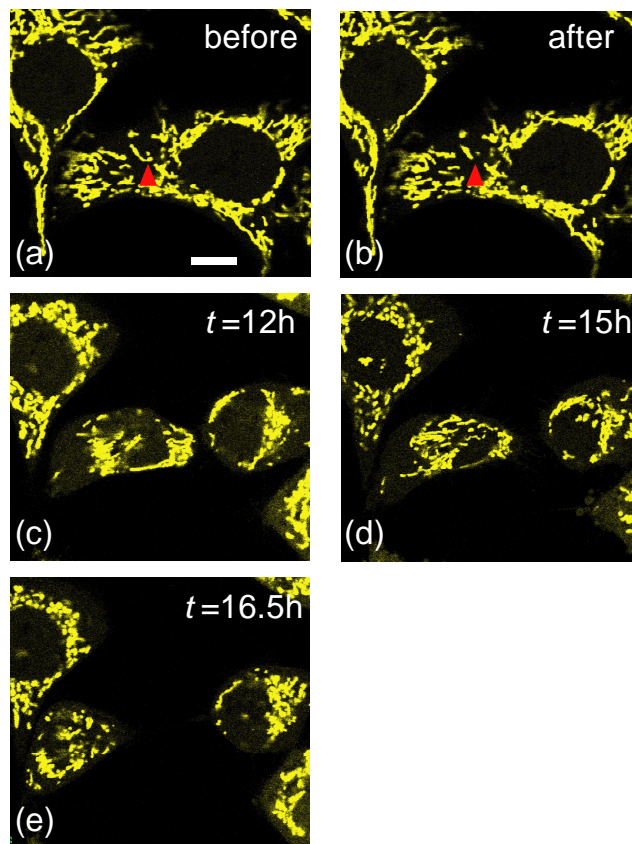


Fig. 5. Cell division after femtosecond laser disruption of a mitochondrion labeled with EYFP. Confocal images (a) before and (b) after femtosecond laser irradiation with 0.39 nJ/pulse (exposure time: 32 ms). The red arrow indicates the irradiation point. (c-f) Time-lapse confocal images. The process of cell division finished successfully 12 h after laser irradiation (c-d). The migration of daughter cells was observed from 12 to 16.5 h after laser irradiation (f). Scale bar: 10 μ m.

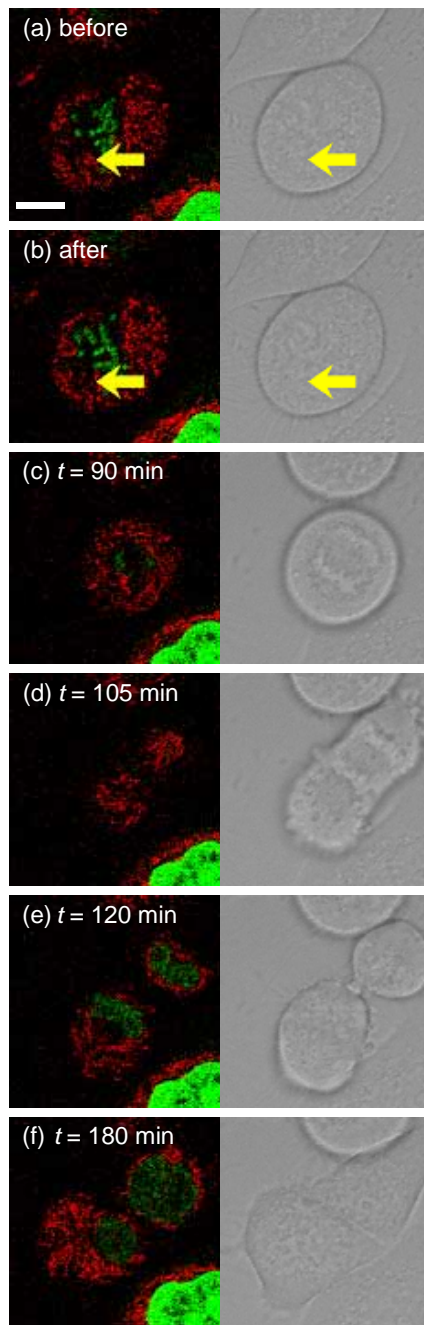


Fig. 6. Mitotic events of cell division after disruption of mitochondria in the histone EGFP-H1 expressed cell. The disruption of a single mitochondrion by femtosecond laser irradiation had no influence on cell division or cell activity. The cell nuclei and mitotic chromosomes in HeLa cells were visualized using histone EGFP-H1. Mitochondria were stained with MitoTracker Red. Confocal fluorescence image and transmission image (a) before and (b) after femtosecond laser irradiation with 0.39 nJ/pulse (exposure time: 32 ms). The yellow arrow indicates the irradiation point. (c)-(f) Time-lapse confocal images and transmission images. The mitotic events of cell division in the irradiated cells proceeded normally. Scale bar: 20 μ m.

To confirm whether or not mitotic events of the cell division proceed normally after laser irradiation, we performed disruption of mitochondria in a histone EGFP-H1 expressed cell. Mitochondria in the HeLa cell were stained with MitoTracker Red. Femtosecond laser pulses at an energy of 0.39 nJ/pulse (exposure time: 32 ms) were irradiated into a single mitochondrion in the synchronized HeLa cell at the prometaphase when mitotic chromosomes start to condense. Figures 6(a) and (b) show the confocal fluorescence image and one-photon transmission image obtained using the Ar⁺ laser before and after irradiation. After femtosecond laser irradiation, we performed long-term observation of the cell at intervals of 5 minutes. At anaphase, the chromosomes split into two sister chromatids and then separated to opposite poles [Fig. 6(c)]. At telophase, the nuclear envelope reformed and a cleavage furrow appeared [Fig. 6(d)]. At cytokinesis, constriction occurred between two separated cells [Fig. 6(e)]. Finally, the cell division completed and two daughter cells were flattened again [Fig. 6(f)]. Our time-lapse observation of irradiated cells revealed that the mitotic events of cell division proceeded normally. Normal cell locomotion was also observed, suggesting that the disruption of a single mitochondrion by femtosecond laser irradiation had no influence on cell activity or cell division. However, the duration of cell division of the irradiated cell was around 3 h, whereas that of normal cells is around 1 h. We have therefore demonstrated the feasibility of femtosecond laser disruption of a mitochondrion without compromising cell viability.

5. Discussion

Although numerous femtosecond-laser-based surgical techniques on biological tissue and subcellular organelles have been demonstrated, the physical mechanisms involved have not been studied in detail. Figure 4 showed that the disruption energy of the labeled mitochondria depends on the fluorescence label. The energy required to disrupt mitochondria labeled with EYFP was smaller than that to disrupt mitochondria labeled with MitoTracker Red; however, the maximum wavelength of two-photon excitation and the two-photon cross section when using EYFP and MitoTracker Red were different [30,31]. The dependence of the dissection of yeast mitotic spindles on laser wavelength has also been reported [24]. The dependence of disruption on the wavelength is still unclear, however, and will be the subject of future work.

In the low-repetition-rate regime (1 kHz), material modification is produced by a single pulse due to the formation of a high-density plasma [15,32]. The free electrons generated by tunnel ionization and multiphoton ionization act as seeds for avalanche ionization, which exponentially increases the free carrier density. The free electrons absorb energy from the electromagnetic field of the laser pulse, leading to laser-induced optical breakdown, the generation of a plasma, and damage to the organelles. In contrast, in a high-repetition-rate femtosecond laser system (typically megahertz order), focusing femtosecond laser pulses in a cell results in an increase in temperature in a localized region surrounding the focal spot through heat accumulation, and material modification occurs due to the formation of a low-density plasma and a cumulative effect [9,33]. As the number of pulses increases, the threshold energy for disruption decreases due to the incubation effect, as seen in Fig. 4. Thermal effects could account for the decreased threshold energy for disruption more effectively than the use of kilohertz pulses.

In multi-photon excitation microscopy, the heating does not play a destructive role [34], and long-term cell viability has been reported [11-14]; however, the energy required for disruption is higher than that for multiphoton-excitation microscopy, and the resulting heat accumulation becomes important. Irradiation with 80-MHz femtosecond laser pulses at higher energy was found to cause impaired cell division, generation of giant cells, and apoptosis-like death [35,36]. However, in the present study, after disruption of a mitochondrion with 76-MHz laser pulses, the irradiated cells did not show loss of viability. Our experiments demonstrated, therefore, that the femtosecond laser oscillator is useful for laser nanosurgery of subcellular organelles without compromising the long-term viability of cells.

The cells divided properly after laser irradiation, although it took longer than normal cell division. These results suggest that the cells can survive after disruption of mitochondria. It has been reported that when microtubules are damaged and cannot associate with kinetochores, spindle checkpoint prevents cell cycle progression [37]. Once the microtubule damage is repaired, the cell enters the anaphase. In our current study, anaphase onset delay was observed after the laser irradiation, suggesting that microtubules adjacent to mitochondria might be damaged by laser irradiation, and cell cycle delay at metaphase was caused by activation of spindle checkpoint. Although it took longer than normal cell division, irradiated cells divided properly. Thus, the disruption of subcellular organelles by femtosecond laser irradiation does not cause cell death. Moreover, irradiated cells preserve their basic function, such as damage repair, energy production, and proliferation.

We also observed mitochondrial fragmentation when the laser pulses were irradiated onto the endoplasmic reticulum (ER). In contrast, we could not detect any morphological change of mitochondria when the laser pulses were irradiated onto the nucleus. Since a common function of the mitochondria and the ER is the storage of calcium (Ca^{2+}), we hypothesize that Ca^{2+} plays an important role in inducing mitochondrial fragmentation. A release of cytochrome C and mitochondrial fragmentation are found at almost the same time in the early stage of apoptosis. Recently, it has been reported that the initial leakage of a dynamin-like GTPase, OPA1, with the release of cytochrome C leads to structural alternation of the mitochondria and an increase in the fragmentation by blocking mitochondrial fusion [38]. It is possible that the laser irradiation promotes the release of OPA1 from the mitochondria. As the irradiation time increased at a given energy, the rate of fragmentation increased. Because megahertz pulse trains were applied, thermal effects may play an important role in mitochondrial fragmentation. In addition, we also observed fragmentation of mitochondria when using kilohertz pulses. The precise physical mechanism responsible for mitochondrial fragmentation is still under investigation.

6. Conclusion

We have demonstrated that focused femtosecond laser pulses from a Ti:sapphire oscillator can selectively disrupt a targeted mitochondrion. The long-term viability of the cells after femtosecond laser irradiation was verified by the observation of cell division and by the presence of cytoplasmic streaming. These experiments demonstrate that a femtosecond laser oscillator can be used to remove a specific organelle from living cells without compromising the long-term viability. Therefore, the femtosecond-laser-based disruption technique has the potential to elucidate functional interactions between organelles. We believe that this technique will find numerous applications in the study of cellular and organelle function.